



Site response and vulnerability index estimation for  
King Saud University Compound, Riyadh, Saudi Arabia.

Prepared by:

Fahad I. Al-Mansour

434101632

Advisor:

Dr. Sattam Abdulkareem Madani

Department of Geology  
College of Science - King Saud University  
(2017)

## **ABSTRACT**

Microtremors measurement at King Saud University compound were performed at 45 sites using Taurus digital seismograph equipped by 3-component trillium compact seismometer with measurement spacing of 400 meters. The recording time continued for 61 minutes at each site with sampling rate of 100 Hz. Then these data were processed and analyzed to estimate the fundamental frequency and the average amplification factor and the vulnerability index as well for all measurements sites.

The results showed that the range of Fundamental frequency in the study area is between 0.64 and 1.94 Hz with average below of 1 Hz. Spectral ratio of H/V ranges from 1.19 to 17.22. Moreover, the seismic vulnerability index at each measurement site was estimated. The seismic vulnerability index ranges from 0.7 to 150. The northern zone is highly vulnerable due to the great thickness of the soft sediments. These results correlate well with the geotechnical borehole data. Based on these results it is concluded that King Saud University compound has low to moderate potential of seismic risk.

## **ACKNOWLEDGMENTS**

I would like to express my deepest appreciation and my grateful thanks to my advisor Dr. Sattam Abdulkareem Madani and Prof. Kamal Hassanein, for the guidance and helpful orientation that given to me during field excursion data processing and writing this report.

I would like also to thank the department of Geology, College of Science - King Saud University for allowing me this opportunity.

## TABLE OF CONTENTS

|                             | Page |
|-----------------------------|------|
| ABSTRACT .....              | 2    |
| ACKNOWLEDGEMENTS .....      | 3    |
| LIST OF FIGURES .....       | 5    |
| LIST OF TABELS .....        | 6    |
| 1. INTRODUCTION.....        | 7    |
| 1.1 LITERATURE REVIEW.....  | 7    |
| 2. GEOLOGICAL SETTING ..... | 8    |
| 3. METHODOLOGY.....         | 11   |
| 4. DATA ACQUISITION .....   | 11   |
| 5. DATA PROCESSING.....     | 21   |
| 6. RESULTS .....            | 24   |
| 7. CONCLUSIONS.....         | 31   |
| 8. REFERENCES.....          | 32   |

## LIST OF FIGURES

|   | Page |
|---|------|
| FIGURE 1. Geological of the study area (ArcMap) .....           | 10   |
| FIGURE 2. Trillium sensor directed to the north pole .....      | 12   |
| FIGURE 3. Taurus the digital seismograph .....                  | 12   |
| FIGURE 4. Location of the study area (ArcMap) .....             | 14   |
| FIGURE 5. Sequence of the H/V spectral ratio of point M19 ..... | 23   |
| FIGURE 6. Fundamental frequency ( $f_0$ ) contour map .....     | 26   |
| FIGURE 7. Amplification factor ( $A_0$ ) contour map .....      | 27   |
| FIGURE 8. Vulnerability index ( $V_i$ ) contour map .....       | 28   |
| FIGURE 9. H/V ratio curve for all measuring points .....        | 30   |

## LIST OF TABLES

|  | Page |
|--|------|
| TABLE 1. Location and duration time of the measuring points..... | 15   |
| TABLE 2. Test boring for Borehole 2.....                         | 16   |
| TABLE 3. Test boring for Borehole 3.....                         | 17   |
| TABLE 4. Test boring for Borehole 4.....                         | 18   |
| TABLE 5. Test boring for Borehole 5 page 1.....                  | 19   |
| TABLE 6. Test boring for Borehole 5 page 2.....                  | 20   |
| TABLE 7. Data processing parameters of measuring points.....     | 25   |

## **1. Introduction**

Microtremor is a ground vibration (Susilo and Wiyono, 2012) caused by natural or artificial events, such as wind, waves, or vibrations of a vehicle that can reflect the geological conditions near the surface. The study aims to assist the site response effect by calculating the Microtremor measurements to identify the vulnerable sites within the King Saud University compound, Riyadh, Saudi Arabia (Fig.4).

The methods applied in this study are microtremor data which carried out including analysis of H/V amplification ratio, dominant frequency and seismic vulnerability index. The results after proccing matched with the geotechnical reports about four boreholes that were drilled to depths varying from 8 to 12 m below the existing ground surface (Soil & Foundation Co. Ltd., 2014; Fig. 1).

### **1.1 Literature Review**

Ventura et al. (2006) Site Period Estimations Using Microtremor Measurements- Experimental and Analytical Studies in British Columbia, this paper presents site period investigations at nodes on a 1-km grid within a 6-km by 8-km area in Vancouver and Richmond, BC. The area includes a range of site conditions, and is selected as the pilot application area for an urban seismic instrumentation project (Canadian Urban Seismology Program - CUSP) undertaken by the Geological Survey of Canada (GSC).

Noor and Daud (2016) Determination of Soil Thickness Based on Natural Frequency Using Microtremor Measurement ambient vibrations from microtremor measurement were carried out in the Universiti Tun Hussein Onn Malaysia (UTHM) using Lennartz 1Hz tri-axial seismometer sensor. Microtremor measurements have been conducted on 5 boreholes at UTHM, to study the correlation between the natural frequency ( $F_0$ ) and depth of borehole.

Fnais et al. (2010) Microtremor measurements in Yanbu city of Western Saudi Arabia: A tool for seismic microzonation, Microtremor measurements are one of the most popular world-wide tool for estimation of site response especially within the urban area. This technique has been applied over 85 sites distributed regularly through Yanbu metropolitan area with an aim of seismic hazard microzonation for ground shaking site effects.

## 2. Geological Setting

The study is conducted in King Saud University compound, Riyadh, most of the compound lay on Arab Formation Member C and D, also there near the study site the Late Jurassic Jubaila Limestone (Arkell, 1952), divided by Manivit et al. (1985) into informal units J1 and J2, with alluvium and sheet gravel also nearby.

Map of the study sites in (Fig.1). The Arab Formation (Veslet et al., 1991), formally defined by Steineke et al. (1958), was revised by Powers et al. (1966) and Powers (1968), who described a subsurface alternation, 127.5 m thick (Dammam well7), of limestone and anhydrite, subdivided into four formal members from Arab-D at the bottom to Arab-A at the top. Each member corresponds to a sedimentologic sequence that evolves from shallow-water marine limestone at the base to anhydrite at the top. The anhydritic part of the Arab-A Member, however, is more than 90 m thick, and Powers et al. (1966) therefore assigned it formation status.

Rocks assigned to the Arab-D Member in the Riyadh quadrangle are predominantly carbonate. Collapse breccias overlying this first carbonate unit of the formation are also regarded as part of the member; however, as they usually constitute the foot of the cuesta of Arab-C carbonates, they are mapped together with Arab-C Member carbonates. Outcrop thicknesses of the Arab-D Member (including carbonates and breccia) range from 27 m in the central part of the quadrangle to 20.50 m in the northwest, and 17 m in the south.

The carbonate facies of the Arab-D Member, 12m thick east of Al Ha'ir, comprises an alternation of gray to bluish laminated calcareous mudstone and bioclastic, in- traclastic, and locally oolitic calcarenite that channels the muddy facies. Beige micropelletoidal laminated limestone and gypsiferous laminae showing secondary calcitization occur in the upper part of the sequence.

The evaporitic part of the Arab-D Member is not known in outcrop. Solution breccias enveloping components of the Arab-D and Arab-C members are assigned to a lower breccia complex which is 25 m thick east of Al Ha'ir, and 13 m thick at Manffihah in the south of the city of Riyadh. The lower breccia complex is composed of angular fragments of various types of limestone and bioclastic calcarenite, the size of the fragments increasing from the base (a few centimeters) to the top (several decimeters). The breccia cement is entirely calcitized from a former gypsiferous matrix. Locally, in the Awsat graben area, fine-grained sandstone in channels 10 to 50 m wide and 2 to 10 m thick, showing secondary silicification, has been disaggregated



and occurs in the lower breccia complex over about 100 m: the direction of the channel flow is generally northeasterly.

In the Abfi Jifan oil field, the evaporitic facies of the Arab-D Member comprise 35.66m of gray to white massive anhydrite.

The subsurface geologic information is based on the geotechnical reports about four boreholes that were drilled to depths varying from 6 to 15 m below the existing ground surface (Soil & Foundation Co. Ltd., 2014; Fig. 1). The subsurface geologic setting at the site consists of three layers that extend from the ground surface to the maximum depths investigated:

- Silty sand with gravel: A top layer of brown medium dense and dry to damp silty sand with gravel. This layer has an average thickness of ~5.5 m.
- Completely weathered limestone: Below the top layer of the very dense sand; dry to damp and creamy; completely weathered limestone in four boreholes. The thickness of this layer varies from 2.5 to 13.5 m.
- Limestone: Below the top layer in the BH-3borehole. It is interbedded with thin layers of silty sand; creamy, moderately weathered, and very highly to highly fractured limestone rock.

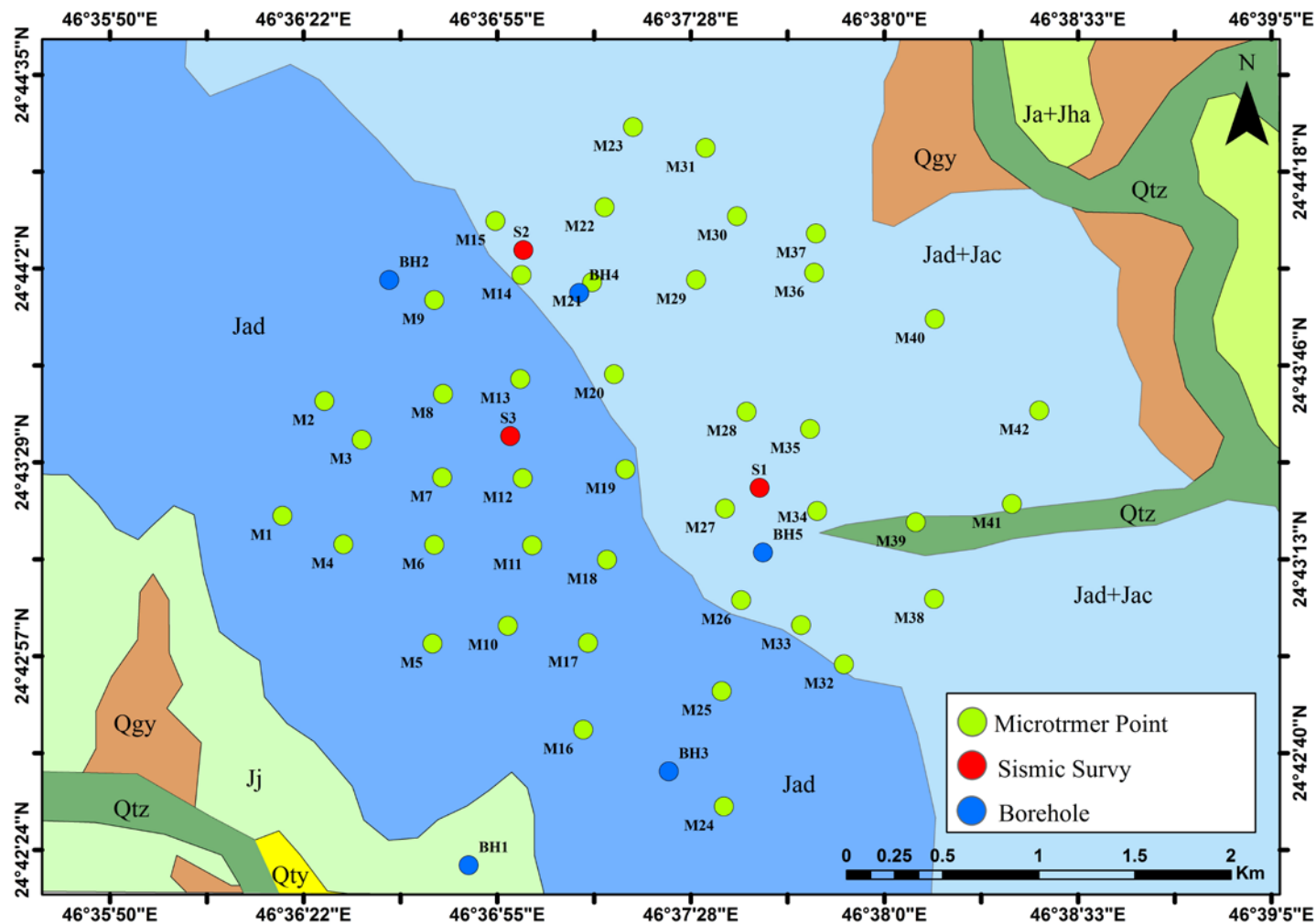


**Figure (1) Geological of the study area (ArcMap).**

### **3. Methodology**

The methods applied on this study are evaluation on geological and seismological secondary data. Evaluations on microtremor data is also carried out including analysis of H/V amplification ratio, dominant frequency and seismic vulnerability index.

Microtremor is a ground vibration (Susilo and Wiyono, 2012) caused by natural or artificial events, such as wind, waves, or vibrations of a vehicle that can reflect the geological conditions near the surface. Microtremor is used in seismic techniques to estimate the shear wave velocity profile ( $V_s$ ). Microtremor also dominated by surface waves that can be used to determine the Rayleigh wave dispersion curve without the need for an artificial source. Microtremor analysis can be performed using HVSr method (Horizontal to Vertical Spectral Ratio). This method is one of the easiest and most inexpensive ways to understand the properties of the subsurface layer structure without causing disruption to the structure.

HVSr method is a method that is used as an indicator of subsurface structure, which shows the relationship between the ratio of the spectrum of H/V with the ellipticity curve of Rayleigh waves. The H/V is the ratio between the amplitude of Fourier spectral of horizontal and vertical components of microtremor. Many urban areas with large populations are erected on soft-sediment, the soil structure tends to amplify the seismic waves. The soft lithology tends to respond a long period of vibration (low frequency), and vice versa.

### **4. Data Acquisition**

#### **4.1 Microtremor Measurement**

Microtremor data acquisition has been collected using Taurus digital seismograph (Nanometrics Company) equipped with three-component Trillium compact seismometer. These data acquired during from the period of 2 -15 February 2017. The total sites of measurements are 45 distributed all over the study area (Table 2) with spacing 400 meters (Fig. 1). The continuous recording period was extended up to 60 minutes with 100 Hz sampling rate at each recording site (360000 samples at each site) following the recommendations of the SESAME project (SESAME, 2004; Bard, 2007).



**Figure (3) Taurus the digital seismograph.**



**Figure (2) Trillium sensor directed to the north pole.**

| Station | Latitude (North) | Longitude (East) | Start Time | End Time | Duration (Hour) |
|---------|------------------|------------------|------------|----------|-----------------|
| M1      | 24.72233         | 46.60523         | 13:43      | 14:44    | 1:01            |
| M2      | 24.72769         | 46.60719         | 15:39      | 16:40    | 1:01            |
| M3      | 24.72589         | 46.60894         | 18:19      | 19:20    | 1:01            |
| M4      | 24.721           | 46.60809         | 7:10       | 8:11     | 1:01            |
| M5      | 24.71636         | 46.61225         | 14:20      | 15:21    | 1:01            |
| M6      | 24.72097         | 46.61233         | 17:24      | 18:25    | 1:01            |
| M7      | 24.72412         | 46.61271         | 19:25      | 20:26    | 1:01            |
| M8      | 24.72803         | 46.61275         | 8:44       | 9:45     | 1:01            |
| M9      | 24.73242         | 46.61233         | 10:56      | 11:57    | 1:01            |
| M10     | 24.71719         | 46.61578         | 13:16      | 14:17    | 1:01            |
| M11     | 24.72094         | 46.61692         | 15:47      | 16:48    | 1:01            |
| M12     | 24.72408         | 46.61647         | 13:20      | 14:21    | 1:01            |
| M13     | 24.72872         | 46.61636         | 14:58      | 15:59    | 1:01            |
| M14     | 24.73358         | 46.61642         | 17:58      | 18:59    | 1:01            |
| M15     | 24.73611         | 46.61519         | 10:30      | 11:31    | 1:01            |
| M16     | 24.71233         | 46.60264         | 12:43      | 13:44    | 1:01            |
| M17     | 24.71639         | 46.61953         | 14:52      | 15:53    | 1:01            |
| M18     | 24.72028         | 46.62042         | 9:12       | 10:13    | 1:01            |
| M19     | 24.7245          | 46.62128         | 11:59      | 13:00    | 1:01            |
| M20     | 24.72894         | 46.62075         | 13:55      | 14:56    | 1:01            |
| M21     | 24.73325         | 46.61972         | 16:09      | 17:10    | 1:01            |
| M22     | 24.73675         | 46.62031         | 18:14      | 19:15    | 1:01            |

|     |          |          |       |       |      |
|-----|----------|----------|-------|-------|------|
| M23 | 24.7405  | 46.62164 | 12:15 | 13:16 | 1:01 |
| M24 | 24.70875 | 46.62589 | 14:02 | 15:03 | 1:01 |
| M25 | 24.71414 | 46.62578 | 16:24 | 17:25 | 1:01 |
| M26 | 24.71839 | 46.62669 | 7:51  | 8:52  | 1:01 |
| M27 | 24.72267 | 46.62594 | 12:21 | 13:22 | 1:01 |
| M28 | 24.72719 | 46.62694 | 13:50 | 14:51 | 1:01 |
| M29 | 24.73336 | 46.62458 | 15:31 | 16:32 | 1:01 |
| M30 | 24.73633 | 46.6265  | 17:08 | 18:09 | 1:01 |
| M31 | 24.73953 | 46.62503 | 18:35 | 19:36 | 1:01 |
| M32 | 24.71539 | 46.6315  | 6:09  | 7:10  | 1:01 |
| M33 | 24.71722 | 46.6295  | 7:28  | 8:29  | 1:01 |
| M34 | 24.72256 | 46.63025 | 8:49  | 9:50  | 1:01 |
| M35 | 24.72639 | 46.62992 | 10:46 | 11:47 | 1:01 |
| M36 | 24.73369 | 46.63011 | 12:15 | 13:16 | 1:01 |
| M37 | 24.73553 | 46.63019 | 13:50 | 14:51 | 1:01 |
| M38 | 24.71844 | 46.63572 | 13:20 | 14:21 | 1:01 |
| M39 | 24.72203 | 46.63486 | 14:39 | 15:40 | 1:01 |
| M40 | 24.73153 | 46.63575 | 9:10  | 10:11 | 1:01 |
| M41 | 24.72289 | 46.63936 | 10:45 | 11:46 | 1:01 |
| M42 | 24.72725 | 46.64064 | 12:07 | 13:08 | 1:01 |
| S1  | 24.72364 | 46.62756 | 13:37 | 14:38 | 1:01 |
| S2  | 24.73475 | 46.6165  | 15:09 | 16:10 | 1:01 |
| S3  | 24.72606 | 46.61589 | 17:26 | 18:27 | 1:01 |

**Table (1) Location and duration time of the measuring points.**



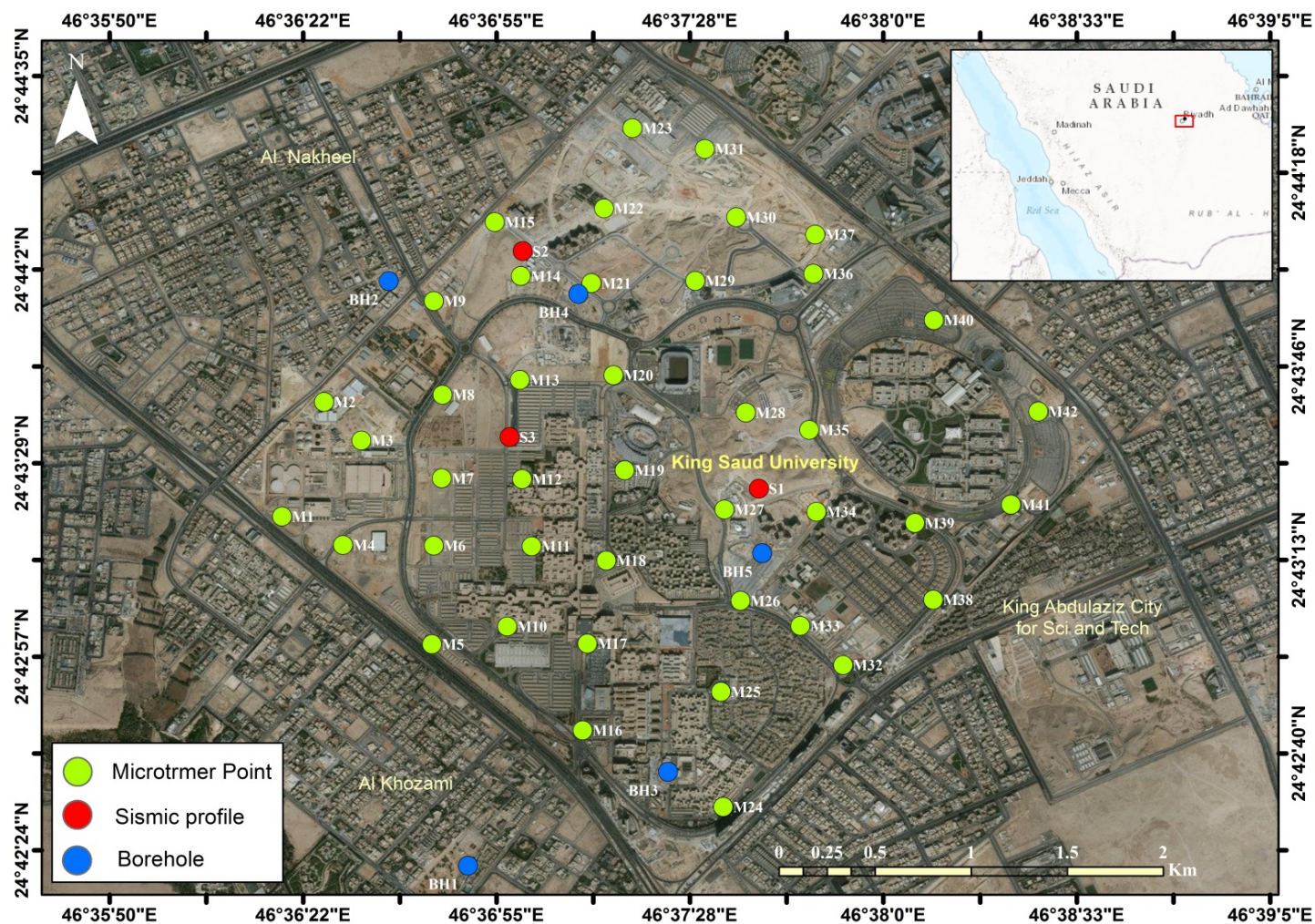
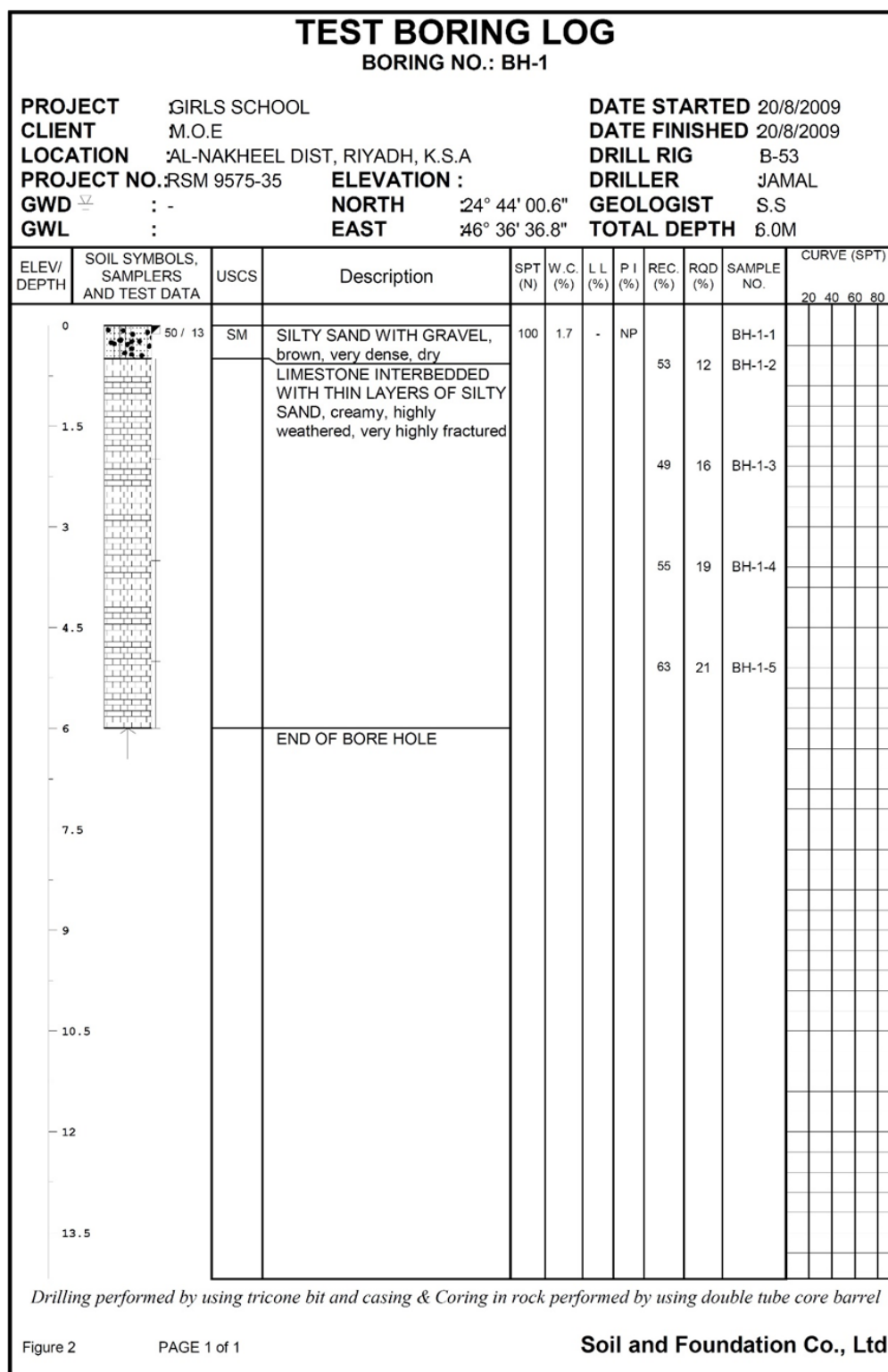


Figure (4) Location of the study area (ArcMap).

## **4.2 Borehole Collection**

The report from Soil & Foundation Co. Ltd. (2014) presents the results of geotechnical investigation carried out by Geotechnical and Material Testing Division of The Saudi Engineer.

The purpose of the geotechnical investigation was to determine the subsurface formation and ground water conditions to evaluate the allowable bearing capacity of the subsurface formation encountered at the site and to recommend the most feasible type of foundation for the proposed structure. Four Boreholes were performed at the site. The boreholes 2 and 3 were drilled to 6 m depth while the borehole 4 to 7.5 m depth and the borehole 5 to 15 m depth, the subsurface geologic setting at the site consists of three layers.



**Table (2) Test boring for Borehole 2 (Soil & Foundation Co. Ltd., 2014).**



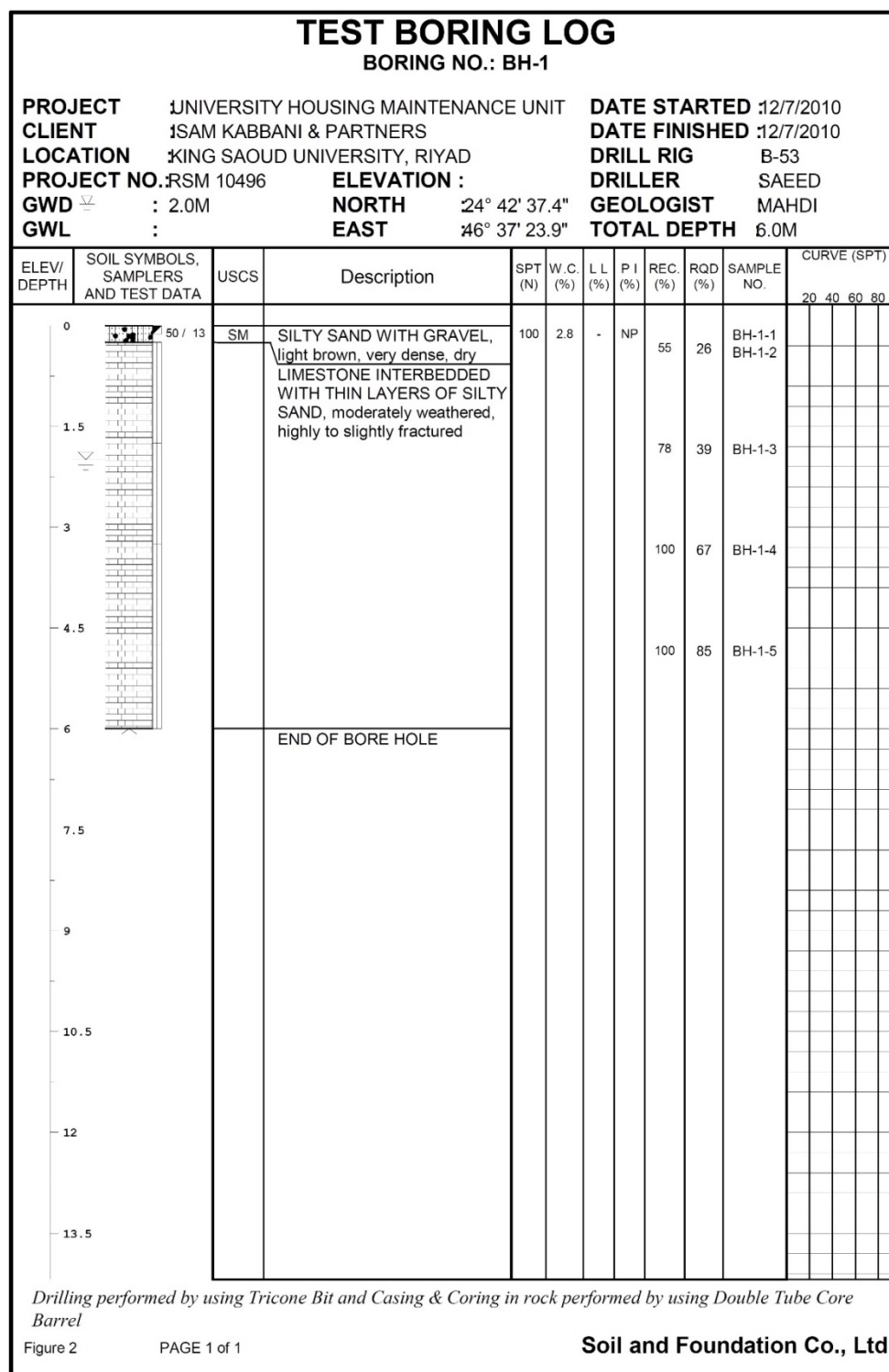


**Table (3) Test boring for Borehole 3 (Soil & Foundation Co. Ltd., 2014).**

# TEST BORING LOG

BORING NO.: BH-1

PROJECT HEADQUARTER OF SAUDI ECONOMY

CLIENT AL-FAYADH

LOCATION K.S.U., RIYADH, K.S.A

PROJECT NO. RSM 11282

ELEVATION :

GWD : 4.3m

NORTH 24° 43' 57.9"

GWL :

EAST 46° 37' 08.8"

DATE STARTED 28/2/2012

DATE FINISHED 28/2/2012

DRILL RIG B-53

DRILLER SAEED

GEOLOGIST MAHDI

TOTAL DEPTH 7.5M

| ELEV/<br>DEPTH | SOIL SYMBOLS,<br>SAMPLERS<br>AND TEST DATA | USCS | Description  | SPT<br>(N) | W.C.<br>(%) | L.L.<br>(%) | P.I.<br>(%) | REC.<br>(%) | RQD<br>(%) | SAMPLE<br>NO. | CURVE (SPT) |
|----------------|--|------|--|------------|-------------|-------------|-------------|-------------|------------|---------------|-------------|
| 0              | 3 / 15<br>3 / 15<br>8 / 15                 | SM   | SILTY SAND WITH GRAVEL,<br>brown, medium dense, dry                        | 11         | 1.9         |             |             |             |            | BH-1-1        |             |
| 1.5            | 3 / 15<br>4 / 15<br>9 / 15                 |      |  | 13         | 2.3         | -           | NP          |             |            | BH-1-2        |             |
| 3              |  |      | LIMESTONE, creamy, highly<br>weathered, very highly to highly<br>fractured |            |             |             |             | 25          | 0          | BH-1-3        |             |
| 4.5            |  |      |  |            |             |             |             | 50          | 13         | BH-1-4        |             |
| 6              |  |      |  |            |             |             |             | 60          | 40         | BH-1-5        |             |
| 7.5            |  |      | END OF BORE HOLE   |            |             |             |             | 70          | 47         | BH-1-6        |             |
| 9              |  |      |  |            |             |             |             |             |            |               |             |
| 10.5           |  |      |  |            |             |             |             |             |            |               |             |
| 12             |  |      |  |            |             |             |             |             |            |               |             |
| 13.5           |  |      |  |            |             |             |             |             |            |               |             |

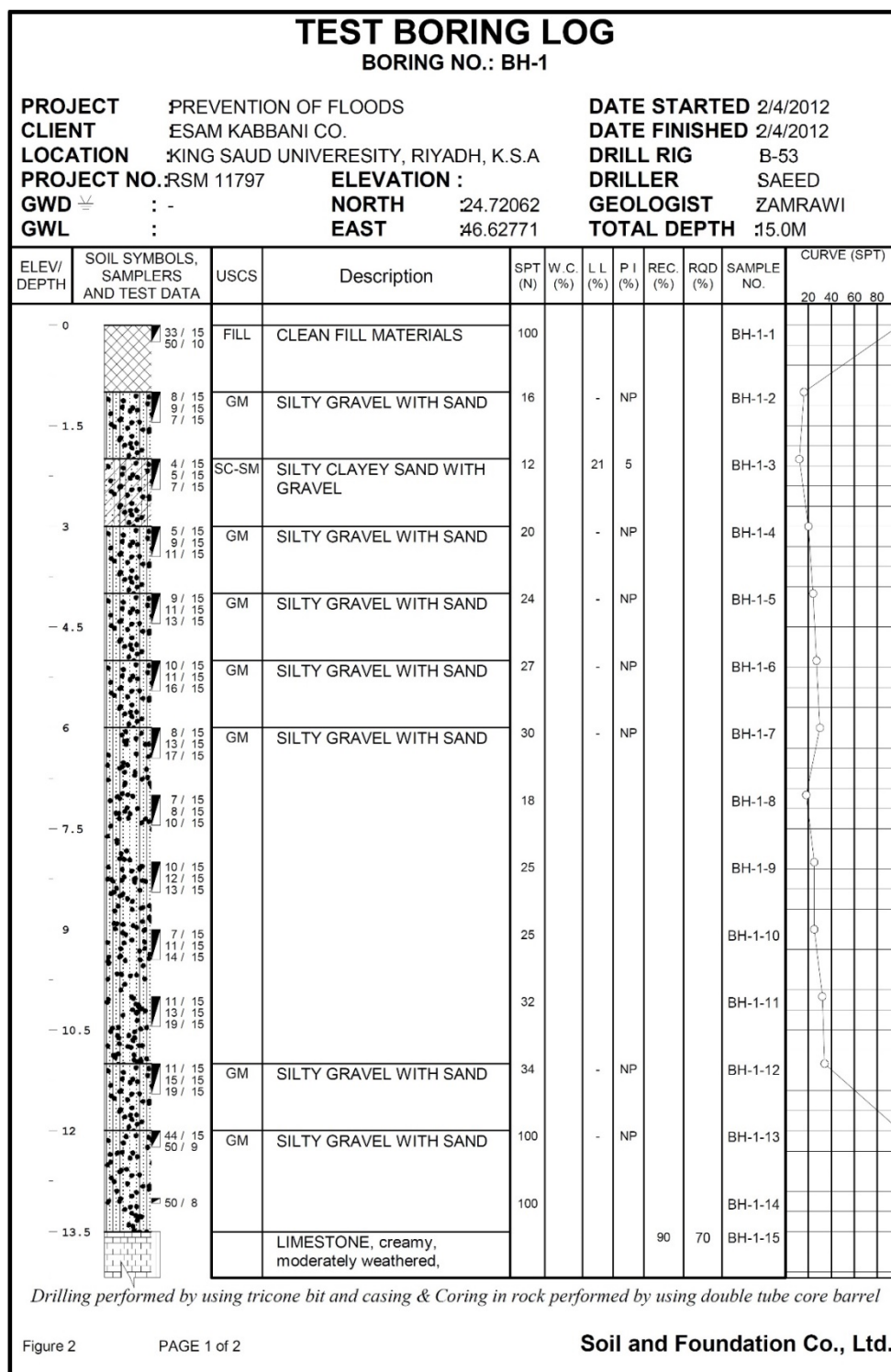
Drilling performed by using tricone bit and casing & Coring in rock performed by using double tube core barrel

Figure 2

PAGE 1 of 1

Soil and Foundation Co., Ltd.

Table (4) Test boring for Borehole 4 (Soil & Foundation Co. Ltd., 2014).



**Table (5) Test boring for Borehole 5 page 1 (Soil & Foundation Co. Ltd., 2014).**

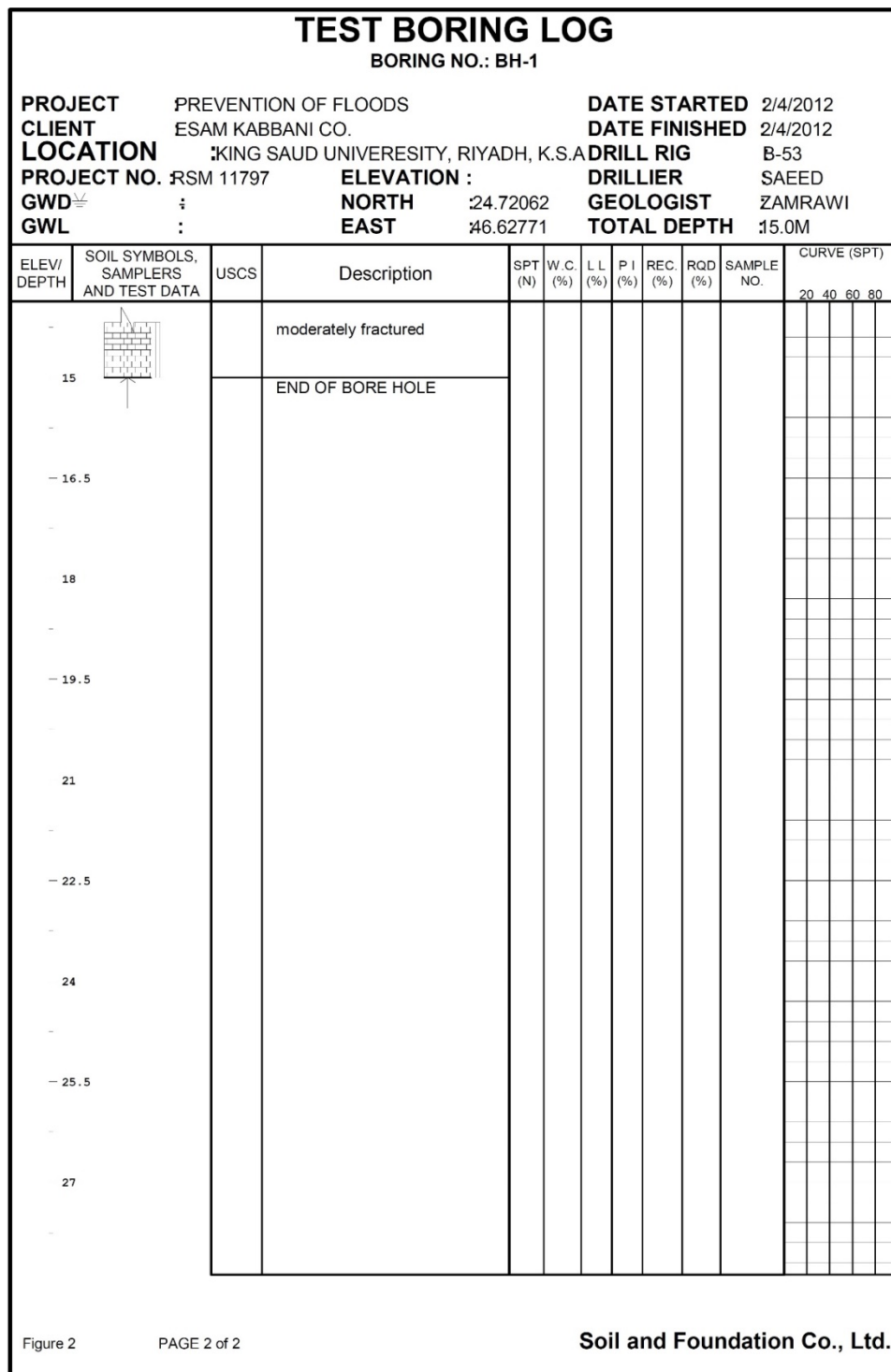


**Table (6) Test boring for Borehole 5 Page 2 (Soil & Foundation Co. Ltd., 2014).**

## 5. Data Processing

The next step is the processing that is composed of the FFT process by Geopsy program, involving the smoothing process. Smoothing process is done by using algorithms Konno and Ohmachi (1998) with bandwidth  $b$  coefficient of 25 second. It is also made the process of cosine taper to minimize the effects of borders or boundaries due to window selection process. Konno-Ohmachi algorithm is stated in the following equation:

$$W_B(f, f_c) = \frac{\sin(\log_{10}(\frac{f}{f_c})^b)}{(\log_{10}(\frac{f}{f_c})^4)}$$

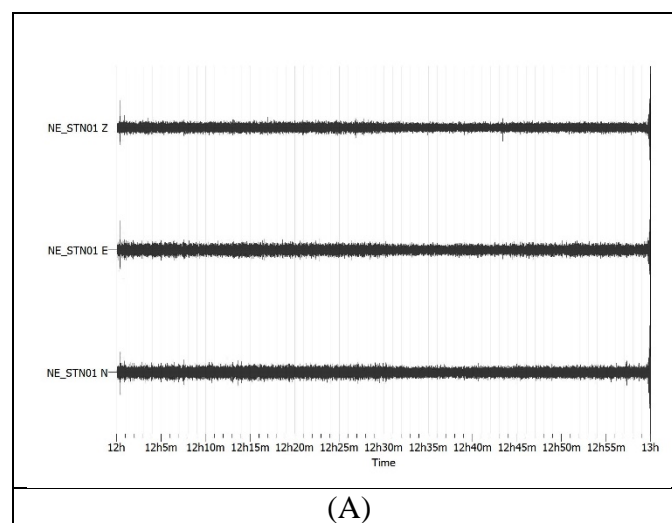
where:

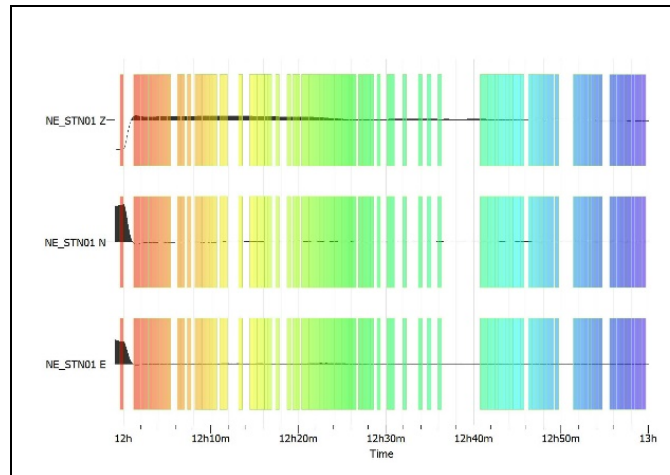
$f$  = frequency

$f_c$  = the central frequency where the smoothing is done

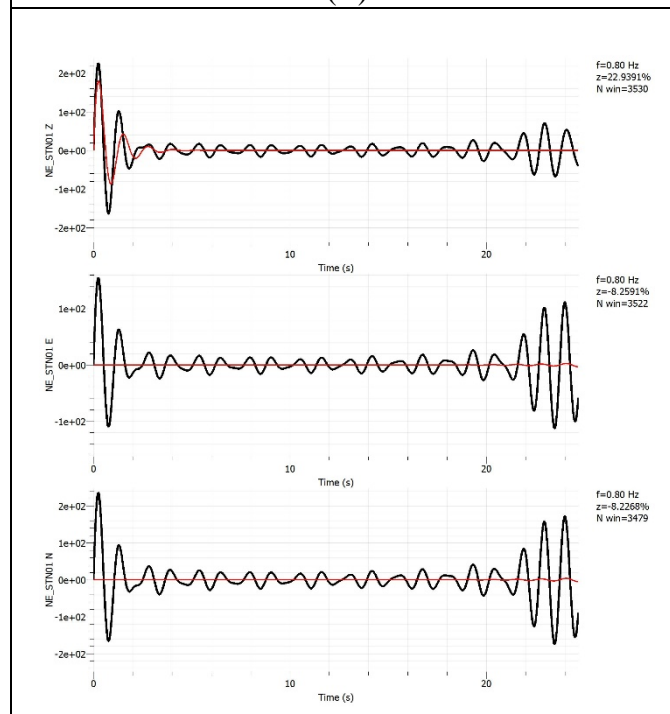
$b$  = bandwidth coefficient

To obtain the spectral ratio of horizontal and vertical components, then the two horizontal components must be one value, using the average of the square, before divided by the horizontal component. This process is performed for every window that is selected. Spectral ratio value of H/V is obtained from the average ratio of H/V of all the selected window. To obtain a low standard deviation, then the value of H/V must be either a value of more than 0.4 because values below 0.4 will have a very high standard deviation.

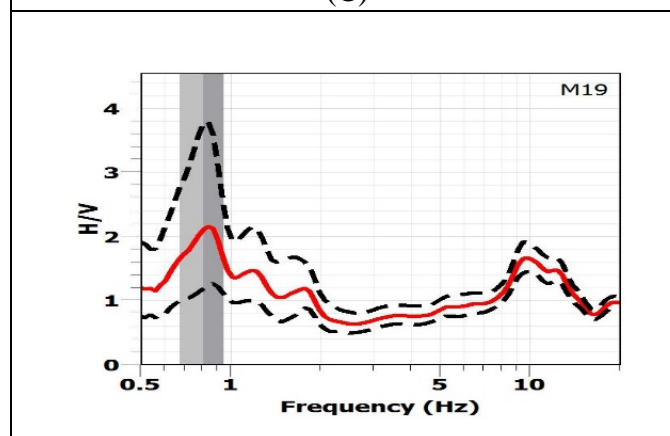




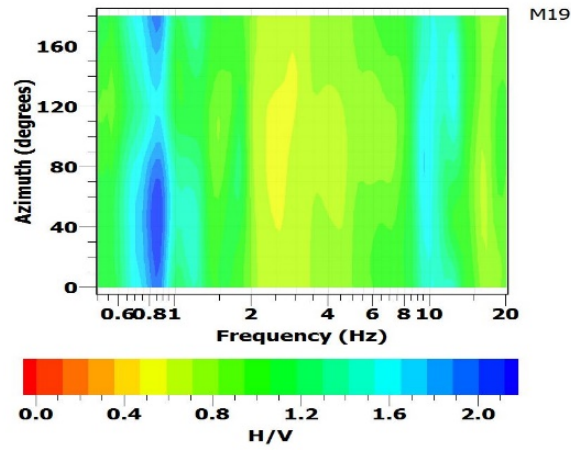
(B)



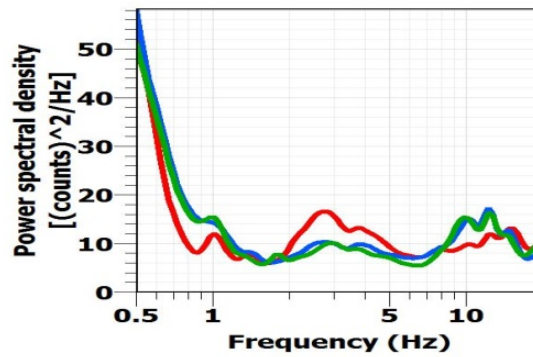
(C)



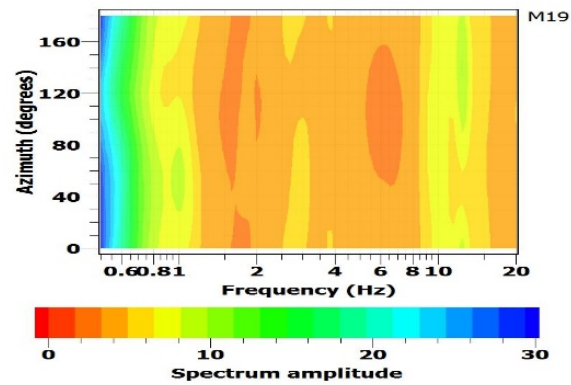
(D)



(E)



(F)



(G)

Figure (5) sequence of the H/V spectral ratio of point M19 (A) show the microtremor record (waveform), (B) show selected windows model, (C) show the damping test of a peak of natural origin 0.81 Hz, (D) H/V ratio curve, (E) show H/V rotate ratio, (F) show the spectrum curve, (G) Spectrum rotate ratio.

## 6. Results

Based on the results of data processing for 45 measuring points (Table 3) ,  $f_0$  values span between 0.64 and 1.94 while  $A_0$  ranges from 1.19 to 17.22 (Fig. 7) . The contour map of  $f_0$  (Fig. 5) illustrates the higher value of the fundamental frequency close to Preparatory Year building which indicates to harder bedrock compared to other areas, also there are another area with moderate  $f_0$  at the old faculty housing.

| Station | $f_0$ | $f_0$ Std. | $A_0$   | $A_0$ Std. | No. of Windows | No. of Cycles |
|---------|-------|------------|---------|------------|----------------|---------------|
| M1      | 0.83  | 0.1564     | 2.12    | 1.92       | 100            | 915000000     |
| M2      | 0.91  | 0.158      | 1.4193  | 1.44       | 102            | 933300000     |
| M3      | 1.25  | 0.3        | 1.33    | 1.86       | 68             | 622200000     |
| M4      | 0.84  | 0.165      | 2.747   | 3.00       | 68             | 622200000     |
| M5      | 0.867 | 0.172      | 1.199   | 1.38       | 111            | 1015650000    |
| M6      | 0.83  | 0.1487     | 3.27    | 2.80       | 61             | 558150000     |
| M7      | 0.709 | 0.123      | 1.7     | 1.64       | 135            | 1235250000    |
| M8      | 0.759 | 0.118      | 12.8729 | 1.83       | 44             | 402600000     |
| M9      | 0.84  | 0.149      | 13.11   | 3.07       | 65             | 594750000     |
| M10     | 0.642 | 0.102      | 2.259   | 2.56       | 46             | 420900000     |
| M11     | 0.7   | 0.122      | 1.862   | 1.94       | 77             | 704550000     |
| M12     | 0.822 | 0.128      | 1.665   | 1.53       | 115            | 1052250000    |
| M13     | 0.8   | 0.15       | 13.52   | 1.73       | 64             | 585600000     |
| M14     | 0.675 | 0.1        | 5.38    | 1.86       | 65             | 594750000     |
| M15     | 0.845 | 0.15       | 5.68    | 2.00       | 55             | 503250000     |
| M16     | 0.785 | 0.1        | 2.7     | 1.73       | 74             | 677100000     |
| M17     | 0.98  | 0.17       | 1.92    | 1.99       | 121            | 1107150000    |
| M18     | 0.944 | 0.158      | 2.03    | 1.71       | 88             | 805200000     |
| M19     | 0.811 | 0.13       | 2.1     | 1.79       | 97             | 887550000     |
| M20     | 1.252 | 0.18       | 4.81    | 1.39       | 90             | 823500000     |
| M21     | 0.92  | 0.17       | 5.55    | 2.26       | 49             | 448350000     |
| M22     | 0.92  | 0.198      | 2.53    | 2.37       | 82             | 750300000     |
| M23     | 1.946 | 0.285      | 2.729   | 2.21       | 97             | 887550000     |
| M24     | 0.77  | 0.127      | 2.72    | 1.79       | 114            | 1043100000    |
| M25     | 1.4   | 1          | 1.3     | 1.27       | 118            | 1079700000    |
| M26     | 0.81  | 0.15       | 4.14    | 1.71       | 82             | 750300000     |
| M27     | 0.88  | 0.198      | 10      | 1.92       | 69             | 631350000     |
| M28     | 0.8   | 0.12       | 11.29   | 1.83       | 71             | 649650000     |
| M29     | 0.8   | 0.13       | 11.55   | 1.71       | 44             | 402600000     |
| M30     | 0.87  | 0.145      | 8.51    | 2.19       | 33             | 301950000     |
| M31     | 0.78  | 0.129      | 12.88   | 1.88       | 40             | 366000000     |
| M32     | 0.776 | 0.144      | 4.36    | 1.92       | 75             | 686250000     |
| M33     | 0.75  | 0.009      | 3.06    | 1.79       | 79             | 722850000     |



|     |       |       |       |      |     |           |
|-----|-------|-------|-------|------|-----|-----------|
| M34 | 0.82  | 0.154 | 3.83  | 1.83 | 58  | 530700000 |
| M35 | 0.84  | 0.14  | 2.95  | 1.99 | 87  | 796050000 |
| M36 | 0.84  | 0.14  | 6.37  | 2.18 | 79  | 722850000 |
| M37 | 0.77  | 0.009 | 17.22 | 1.80 | 38  | 347700000 |
| M38 | 0.829 | 1.14  | 2.48  | 1.27 | 64  | 585600000 |
| M39 | 0.8   | 0.86  | 3.66  | 1.31 | 108 | 988200000 |
| M40 | 0.8   | 0.16  | 3.84  | 1.95 | 77  | 704550000 |
| M41 | 0.758 | 0.125 | 5.4   | 2.11 | 72  | 658800000 |
| M42 | 0.827 | 0.14  | 6.12  | 1.83 | 98  | 896700000 |
| S1  | 0.735 | 0.11  | 6.33  | 2.17 | 79  | 722850000 |
| S2  | 0.72  | 0.119 | 11.71 | 1.75 | 57  | 521550000 |
| S3  | 0.75  | 0.077 | 6.94  | 1.99 | 72  | 658800000 |

**Table (2) Data processing parameters of measuring points.**

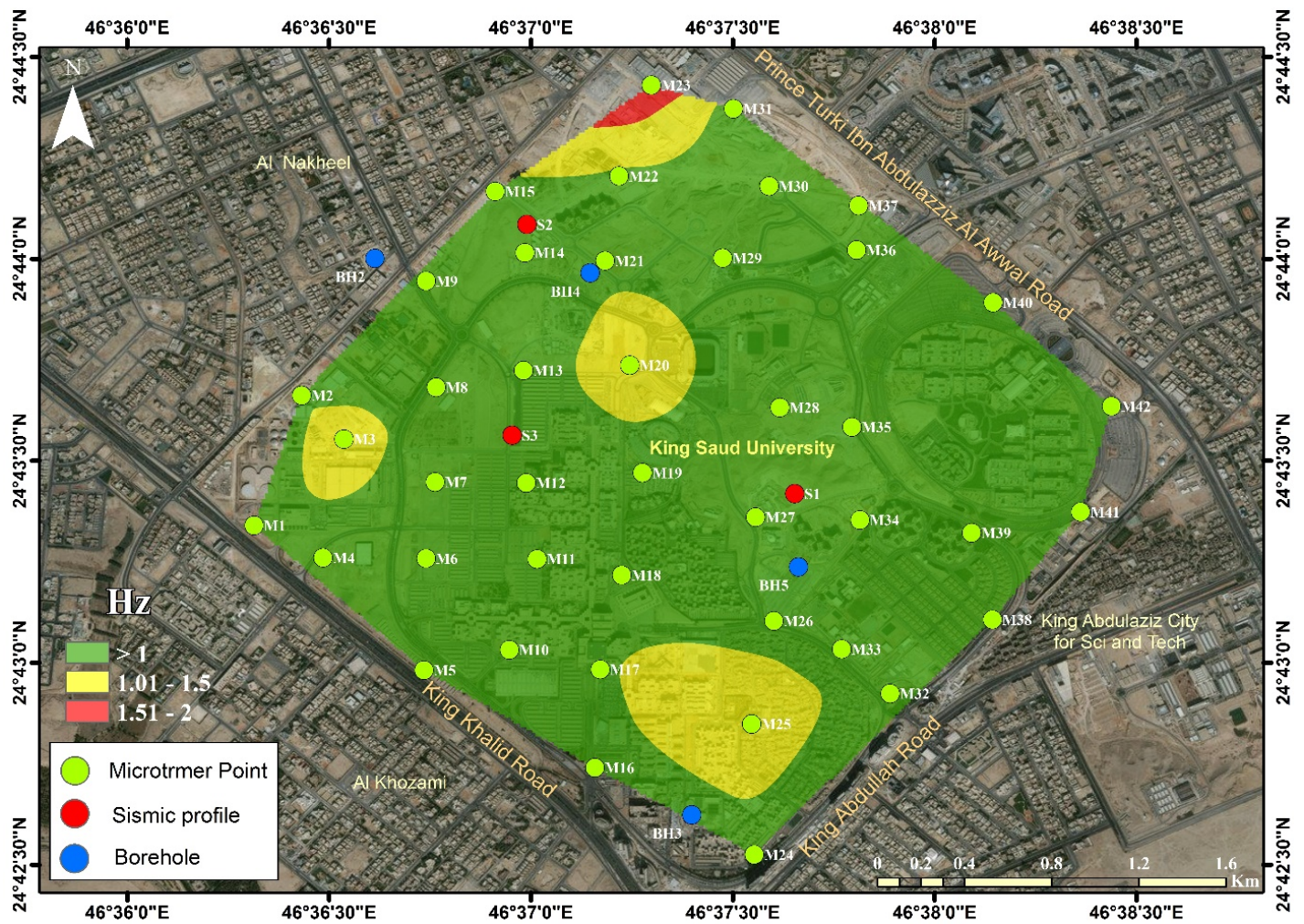


**Figure (6) Fundamental frequency ( $f_0$ ) contour map.**

Contour map of A0 (Fig. 5) shows the higher value of the peak ratio is in the area between M31 and M37 near Prince Turki Ibn Abdulaziz Al Awwal road, while the area from M29 to M27 has moderate A0 values.

The seismic vulnerability index distribution in the area of study has values ranges from 0.7 to 148 (Fig. 6). There are areas which have high susceptibility values (the area between M31 and M37) near Prince Turki Ibn Abdulaziz Al Awwal road.



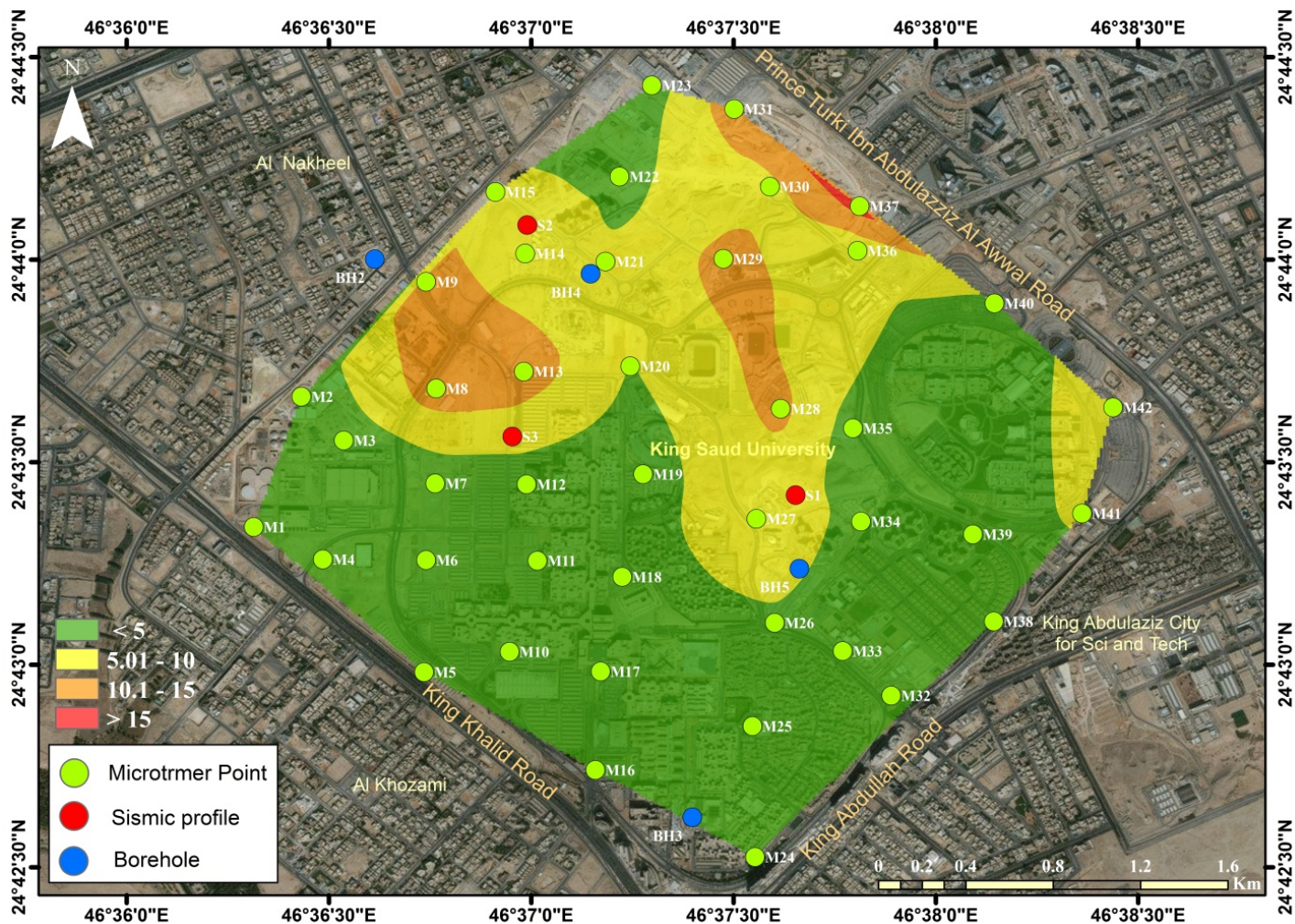
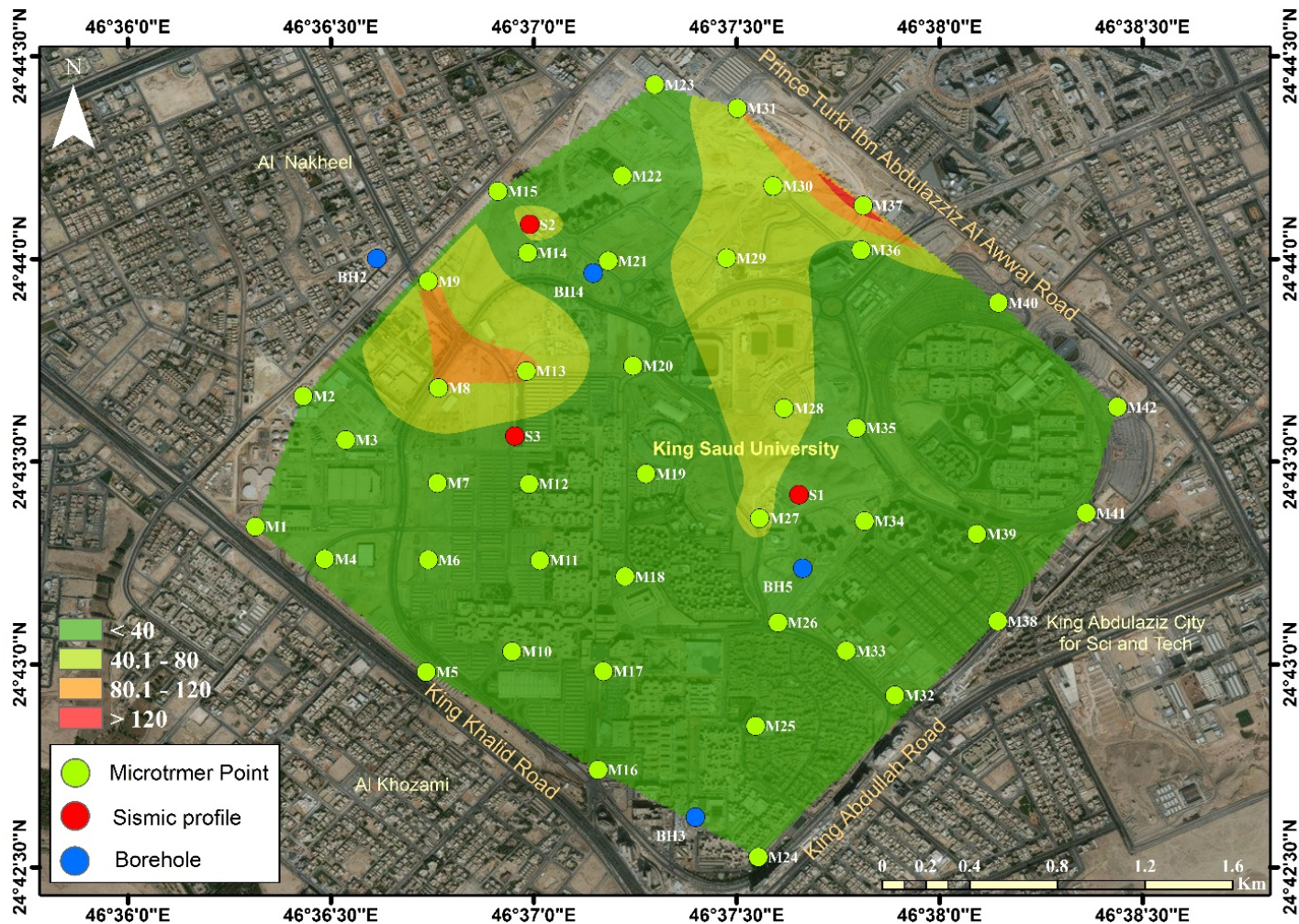
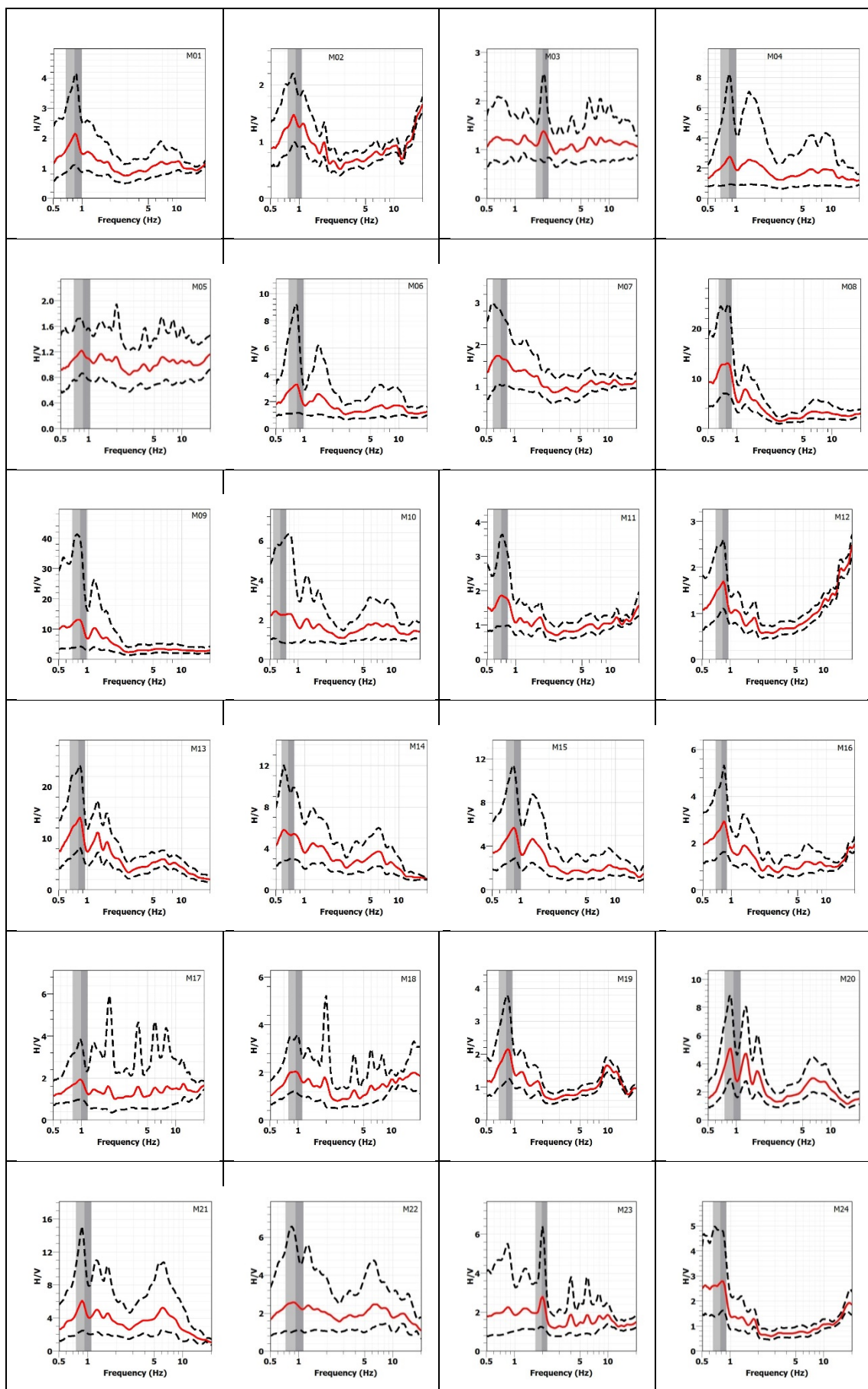


Figure (7) Amplification factor ( $A_0$ ) contour map.





**Figure (8) Vulnerability index (Vi) contour map.**





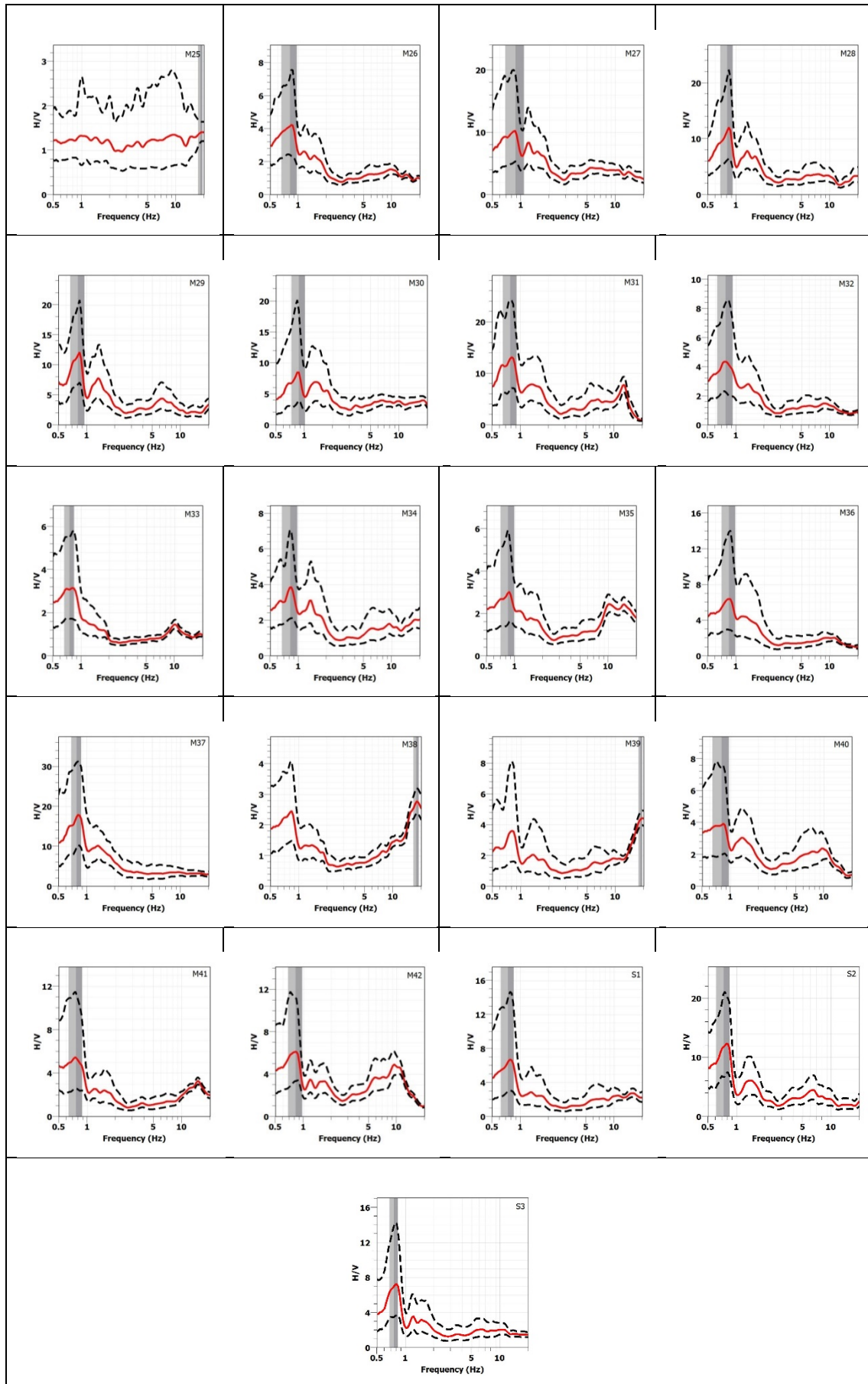


**Figure (9) H/V ratio curve for all measuring points.**

## 7. Conclusions

Based on research results, some conclusions can be outlined as follows:

Fundamental frequency value for KSU compound ranges between 0.64 and 1.94 Hz., while HVSR or amplification factor value varies from 1.19 to 17.22. This corresponds to the value of the seismic vulnerability index ( $K_g$ ) ranges from 0.7 to 148. The geotechnical reports and the results identify the existence of a completely weathered limestone (Soil & Foundation Co. Ltd., 2014). From analysis of these three parameters, it is illustrated that the highest potential will be near the Preparatory Year Building. From the consideration between  $f_0$  and  $A_0$  it is indicated that, the potential damage is quite low.

## 8. References

- Arkell, WJ., 1952, Jurassic ammonites from Jebel Tuwaiq, central central Arabia: Philosophical Transactions of the Royal Society of London, ser. B., vol. 236, p. 241-313.
- Bard, P.Y., 2007, International Training Course on: Seismology, Seismic Data Analysis, Hazard Assessment and Risk Mitigation, Potsdam, Germany, p. 17–22.
- Dunand, F., Bard, P. Y., Chatelain, J. L., Guéguen, P.h., Vassail T. and Farsi, M. N., 2002, Damping and frequency from random method applied to insitu measurements of ambient vibrations: evidence for effective soil structure interaction. 12th European Conference on Earthquake Engineering, London. p. 869.
- El-Asa‘ad, G.M.A., 1984, The paleobiogeographic distribution of the Late Cretaceous fauna of Arabia and surrounding areas: Arab Gulf journal of Scientific Research, vol. 2, no. 1, p. 105-121.
- Konno, K. and Ohmachi, T., 1998, Ground-motion characteristics estimated from spectral ratio between horizontal and vertical components of microtremors: Bulletin of the Seismological Society of America 88, p. 228–241.
- Manivit, J., Pellaton, C., Vaslet, D., Le Nindre, Y.M., Brosse, J.M., Breton, J.P., and Fourniguet, J., 1985, Geologic map of the Darma’ quadrangle, sheet 24 H, Kingdom of Saudi Arabia (with text): Saudi Arabian Deputy Ministry for Mineral Resources, Jeddah, Geoscience Map GM-101A.
- Powers, R.W., 1968, Lexique stratigraphique international: Saudi Arabia: vol. III, Asie, fasc. 10 b 1: Centre National de la Recherche Scientifique, Paris, 177 p.
- Powers, R.W., Ramirez, L.F., Redmond, CD, and Elberg, EL, Jr., 1966, Geology of the Arabian Peninsula: Sedimentary geology of Saudi Arabia: US. Geological Survey Professional Paper, 560-D, 147 p.
- SESAME Project. 2004 Site effects using ambient excitations. URL: <http://sesame-fp5.obs.ujf-grenoble.en>. Accessed on May 1, 2017.
- Soil and Foundation Company, 2014, Geotechnical investigation report for the proposed KACST project, 60 p.
- Susilo, A. and Wiyono, S., 2012, Frequency Analysis and Seismic Vulnerability Index by Using Nakamura Methods at a New Artery Way in Porong, Sidoarjo, Indonesia, International Journal of Applied Physics and Mathematics, Vol. 2, No. 4, P. 227-230.



- Steineke, M., Bramkamp, R.A., and Sander, N.J., 1958, Stratigraphic relations of Arabian Jurassic Oil: American Association of Petroleum Geologists Symposium, Tulsa, U.S.A., p. 1294-1329.
- Vaslet, D., Al-Musllem, M., Maddah, S., Brosse, J.M., Fourniguet, J., Breton, J.P. and Le Nindre, Y.M., 1991, Geologic map of the Ar Riyad quadrangle, sheet 24 I, Kingdom of Saudi Arabia (without Landsat base): Saudi Arabian Deputy Ministry for Mineral Resources. Jeddah, Geoscience Map GM-121 C.